

RSC Advances



This is an *Accepted Manuscript*, which has been through the Royal Society of Chemistry peer review process and has been accepted for publication.

Accepted Manuscripts are published online shortly after acceptance, before technical editing, formatting and proof reading. Using this free service, authors can make their results available to the community, in citable form, before we publish the edited article. This *Accepted Manuscript* will be replaced by the edited, formatted and paginated article as soon as this is available.

You can find more information about *Accepted Manuscripts* in the [Information for Authors](#).

Please note that technical editing may introduce minor changes to the text and/or graphics, which may alter content. The journal's standard [Terms & Conditions](#) and the [Ethical guidelines](#) still apply. In no event shall the Royal Society of Chemistry be held responsible for any errors or omissions in this *Accepted Manuscript* or any consequences arising from the use of any information it contains.

ARTICLE

One-Pot Synthesis of NiAl-CO₃ LDH Anti-Corrosion Coatings from CO₂-Saturated Precursors

Cite this: DOI: 10.1039/x0xx00000x

Yi Liu,^{‡,ab} Tongwen Yu,^{‡,ac} Rui Cai,^{a*} Yanshuo Li,^a Weishen Yang^{a*} and Jürgen Caro^bReceived 00th January 2012,
Accepted 00th January 2012

DOI: 10.1039/x0xx00000x

www.rsc.org/

Anti-corrosive coatings based on layered double hydroxides (LDHs) have been considered as promising alternatives to conventional chromate-containing conversion coatings. Among various LDHs, carbonate-intercalated LDH coatings with *c*-axis preferred orientation should be the optimum structure for protecting metals against corrosion. Herein we successfully prepared NiAl-CO₃ LDH coatings on aluminium plates in one step. Particularly it was found that CO₂ dissolved in the precursor solution exerted great influence on the microstructure and anti-corrosion capacity of prepared LDH coatings. Trace amounts of CO₂ in the precursor solution led to the formation of *ab*-oriented 7 μm-thick LDH coatings, while preferentially *c*-oriented LDH coatings with an average thickness of 12 μm were formed from CO₂-saturated precursor solutions. DC polarization test demonstrated that preferentially *c*-oriented LDH coatings exhibited much higher anti-corrosion performance than *ab*-oriented LDH coatings possibly due to the decreased density of mesoscopic defects. Simultaneously, CO₂, the green gas, was also positively utilized.

Introduction

The Corrosion is the gradual destruction of materials (usually metals) by chemical reaction with their environment. Corrosion of metal and its alloys often leads to a series of economic and safety issues. Chromate-containing conversion coatings, which have historically been evaluated as an effective anticorrosion method for metallic substrates,¹ are currently restricted due to their toxic and carcinogenic properties.² As an alternative, various new materials have been developed.³ Among them, layered double hydroxide (LDH) coatings on metal surfaces provide a cost-effective and eco-friendly way to protect metals (like Mg, Al and their respective alloys) against corrosion.⁴ LDHs are a series of layered compounds consisting of positively charged brucite-like sheets, coupled with charge-compensating anions located in interlayer regions.⁵ Compositional flexibility in both positively charged layers and charge-balancing anions leads to functional diversity.⁶

Using aluminum as a probe substrate, F. Z. Zhang recently reported the synthesis of a laurate-intercalated ZnAl LDH film which involved an anion exchange step.^{4a} The prepared LDH film showed a corrosion current density (abbreviated as I_{corr}) as low as 10^{-9} A·cm⁻² in a direct current (DC) polarization test. X. Duan prepared a ZnAl-NO₃ LDH film⁷ and further revealed that the film not only acted as an anti-corrosive coating but also initiated a self-healing process via the dissolution-recrystallization process upon exposure to a chloride-containing environment.⁸

The most striking feature of LDHs is their compositional flexibility. In terms of anti-corrosive capacity, carbonate-intercalated LDHs should be the optimum choice. This is because the ion-exchange equilibrium constants of charge-compensating anions

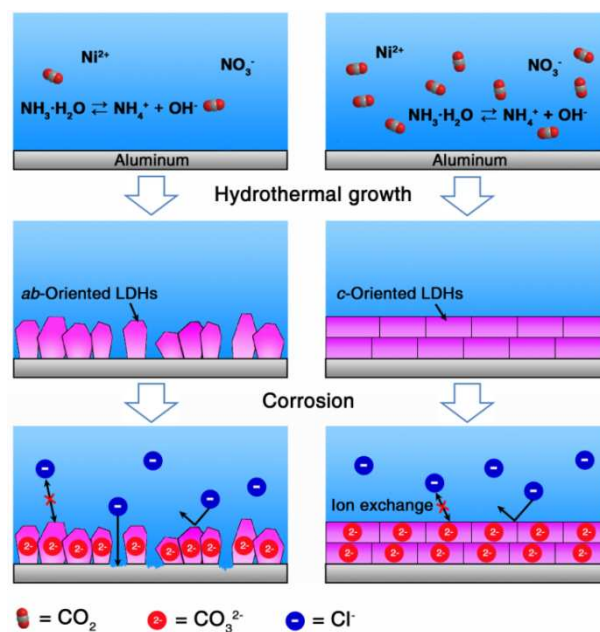


Fig. 1 Schematic illustration of NiAl-CO₃ LDH films prepared from the aged DI water (left) and CO₂-saturated water (right), respectively. Increasing the concentration of dissolved CO₂ in the precursor solution leads to dense LDH films with an enhanced anti-corrosive capacity because the corrosive component (Cl⁻) will not easily exchange the CO₃²⁻ anions located in the interlayer spaces of NiAl-CO₃ LDHs.

follow the sequence $\text{CO}_3^{2-} > \text{SO}_4^{2-} > \text{OH}^- > \text{F}^- > \text{Cl}^- > \text{Br}^- > \text{NO}_3^-$.⁹ In principle, once a carbonate-intercalated LDH film is formed, most of the corrosive components, like the Cl^- , SO_4^{2-} , Br^- and F^- anions commonly found in water, will not easily exchange these carbonate anions, thereby retarding the corrosion of the underlying metals.¹⁰ Besides chemical composition, also the crystallographic orientation of the LDH films may exert a strong influence on their anticorrosive capacity. Under ideal conditions, *c*-oriented LDH films are preferred as corrosion-resistant coatings, because in this case, plate-like LDH crystallites are arranged parallel to the substrate and thus minimize intercrystalline voids and grain boundaries. In particular these boundaries may become inter-crystalline defects upon excessive exposure to the corrosive medium. Inspired by the above-mentioned principles, we report here a one-step, hydrothermal crystallization of preferentially *c*-oriented NiAl-CO₃ LDH coatings on Al substrates. Prepared LDH coatings showed excellent anticorrosive performance, considerable long-term corrosion durability as well as strong mechanical stability (schematically shown in Fig. 1).

Experimental

Synthesis of NiAl-CO₃ LDH films on Al substrates

Pure Al plates were supplied by Aldrich (99.99 wt.%) at a size of $1.5 \times 1.5 \text{ cm}^2$ and a thickness of 0.2 mm.

The precursor solution was prepared by adding 5.8 g $\text{Ni}(\text{NO}_3)_2 \cdot 6\text{H}_2\text{O}$ (98.0 wt.%, Merck) and 4.8 g NH_4NO_3 (98.0 wt.%, Aldrich) into 100 ml CO₂-saturated water (Vitalitas Classic, containing saturated CO₂). Consequently 10 ml $\text{NH}_3 \cdot \text{H}_2\text{O}$ (1 wt.%, Aldrich) was slowly added into the aqueous solution and stirred in an ice bath for 10 min.

An Al plate was first horizontally placed into a 50 ml Teflon-lined stainless vessel. 35 ml of the precursor solution was then poured into the vessel and sealed. The vessel was put into convective oven, pre-heated to 85 °C. After an elapsed time of 40 h, the vessel was taken out and cooled to room temperature in air. Finally the film was washed with copious amounts of Distilled De-Ionized (DDI) water. Before the DC polarization test, the LDH film was dried in a convective oven at 60 °C for 12 h.

Besides CO₂-saturated water, deionized (DI) water was also used as a solvent to prepare LDH films following the same procedure and recipe as shown above. Note: DI water was left in open air for at least 1 month to reach equilibrium of dissolved CO₂ with the surrounding atmosphere.

DC polarization test

We employed a three-electrode system to carry out DC polarization test at room temperature on a Solartron SI 1287 electrochemical interface: NiAl-CO₃ LDH film-coated Al samples or bare Al substrate as a working electrode, a gauze platinum counter electrode, and an Ag/AgCl electrode as the reference electrode.

A 3.5 wt.% aqueous solution of sodium chloride was used as the corrosive medium. Before the test, the samples were immersed in the corrosive medium to measure the open-circuit-potential for 30 min. The sweep rate, potential range of DC polarization test was -1.5 V~+2.5 V (vs. Reference), 10 mV/s. Al plates were supplied by Aldrich (99.99 wt.%) with the size of $1.5 \times 1.5 \text{ cm}^2$ and the thickness of 0.2 mm, respectively.

Results and Discussion

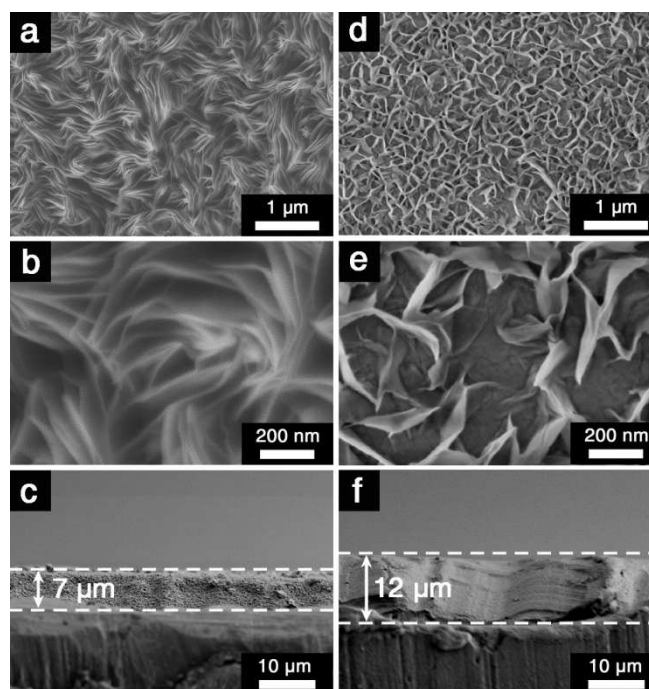


Fig. 2 SEM images of NiAl-CO₃ LDH films prepared from (a, b, c) aged DI water and (d, e, f) CO₂-saturated water solvents, respectively.

Recent studies revealed that NiAl brucite-like sheets had an extraordinarily high affinity for CO₃²⁻ anions derived from dissolved CO₂. For instance, our recent research revealed that the variation of the CO₂ concentration in the precursor solution affected the microstructure and thus gas separation performance of supported NiAl-CO₃ LDH membranes.¹¹ CO₃²⁻ anions located in the interlayer region were derived from CO₂ dissolved in the precursor solution.¹² In our approach, the precursor solution was prepared by mixing $\text{Ni}(\text{NO}_3)_2 \cdot 6\text{H}_2\text{O}$, NH_4NO_3 , and $\text{NH}_3 \cdot \text{H}_2\text{O}$ in a CO₂-saturated H₂O solvent. Then the aluminium substrate, which also served as the Al³⁺ source, was vertically placed into the solution before the chemical bath deposition. It was anticipated that the dissolved CO₂ could act as a source of carbonate anions and participate in the formation of CO₃²⁻ intercalated LDHs. For comparison, aged DI water was also used as the solvent. It was found that the concentration of dissolved CO₂ in the precursor solution exerted significant influence on the microstructure of NiAl-CO₃ LDH coatings. In the case of aged DI water [abbreviated as NiAl-CO₃ LDH (DI aged)], which had a low concentration of dissolved CO₂ ($\sim 1.3 \times 10^{-5} \text{ M}$),¹¹ the Al substrate surface became rough and fully covered with plate-like LDH microcrystals $\sim 1 \mu\text{m}$ in size after the hydrothermal reaction (shown in Fig. 2a). Nevertheless, the formed LDH layer was not well-intergrown. Substantial intercrystalline defects were simultaneously generated and spread over the surface of the LDH film (Fig. 2b). The SEM cross-sectional view from Fig. 2c illustrates that the LDH layer was $\sim 7 \mu\text{m}$ thick. XRD pattern of the film showed five conspicuous diffraction peaks at 2θ values of 11.2°, 22.5°, 34.6°, 60.4° and 61.5° respectively (Fig. 3c), which was consistent with the reflections of (0 0 3), (0 0 6), (0 1 2), (1 1 0) and (1 1 3) crystal planes in NiAl-CO₃ LDH powders (shown in SI-1).¹³ This confirmed that the formed layer indeed belonged to the LDH phase.

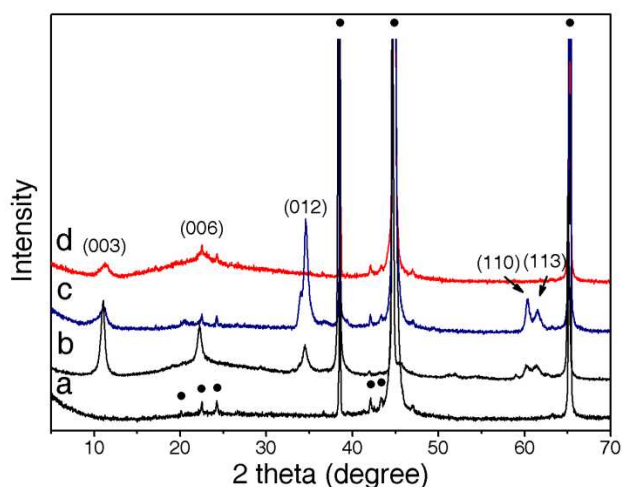


Fig. 3 XRD patterns of (a) bare Al substrate, (b) NiAl-CO₃ LDH powders scraped from NiAl-CO₃ LDH (DI aged) film samples, NiAl-CO₃ LDH films prepared from (c) aged DI water and (d) CO₂-saturated water, respectively. (●) denotes diffraction peaks of the Al substrate phase.

In contrast, the LDH layer synthesized from the CO₂-saturated precursor solution [abbreviated as NiAl-CO₃ LDH (CO₂-satur)], which contained a much higher concentration of dissolved CO₂ ($\sim 3.3 \times 10^{-2}$ M),¹¹ showed a distinct morphology. After *in situ* growth, the Al substrate had been fully covered with well-intergrown LDH crystallites with no visible defects (Fig. 2d), thus indicating that the new layer was highly compact. Higher magnification of the image demonstrated that the LDH crystal faces were well-developed and that the grain size was reduced to ~ 200 nm (Fig. 2e). Nevertheless, the thickness of the LDH layer had reached ~ 12 μ m (Fig. 2f). Different from the NiAl-CO₃ LDH (DI aged) film, only (0 0 3) and (0 0 6) diffraction peaks were found in the whole XRD pattern of the NiAl-CO₃ LDH (CO₂-satur) film (Fig. 3d).

The different morphology of the NiAl-CO₃ LDH (DI aged) and NiAl-CO₃ LDH (CO₂-satur) layers is mainly attributed to the differences in the concentration of dissolved CO₂ in the precursor solution. Owing to the much higher concentration of CO₂ in the CO₂-saturated precursor solution, the concentration of CO₃²⁻, which acts as the intercalating anions, is also higher, which will further increase both the nucleation density and growth rate of the NiAl-CO₃ LDH film (as demonstrated in SI-2).¹¹ In addition, the sufficient supply of CO₂ also effectively suppresses the generation of intercrystalline defects in the NiAl-CO₃ LDH layer during the *in situ* hydrothermal growth. In contrast, substantial defects are formed in the case of aged DI water (Fig. 2a) since the concentration of nutrient CO₂ in the precursor solution is insufficient to guarantee complete sealing of the void spaces in the NiAl-CO₃ LDH (DI aged) layer.

Preferred orientation of NiAl-CO₃ LDH films was further investigated due to its potential impact on the anti-corrosive capacity. The intensity ratio $I_{(0\ 0\ 3)}/I_{(0\ 1\ 2)}$ was employed here to evaluate the preferred orientation of LDH films,⁷ in which $I_{(0\ 0\ 3)}$ and $I_{(0\ 1\ 2)}$ represented peak heights of the (0 0 3) and (0 1 2) diffractions, respectively. A higher $I_{(0\ 0\ 3)}/I_{(0\ 1\ 2)}$ value indicates that the LDH film has a *c*-axis preferred orientation, while a lower value demonstrates that prepared film is preferentially *ab*-oriented. Simultaneously, NiAl-CO₃ LDH powders, which were scraped from corresponding LDH film samples, were also characterized as a reference (Fig. 3b). As was shown in the

figure, all (0 0 3), (0 0 6), (0 1 2), (1 1 0) and (1 1 3) diffraction peaks were clearly observable and the $I_{(0\ 0\ 3)}/I_{(0\ 1\ 2)}$ ratio reached 2.7 for the NiAl-CO₃ LDH powders. As for the NiAl-CO₃ LDH (DI aged) layer (Fig. 3c), this ratio was reduced significantly to 0.2, thus revealing that this film was dominantly *ab*-oriented and most LDH crystallites should be vertically aligned on the substrate (Fig. 2a). Additionally, a strong (1 1 0) diffraction peak at 2θ value of 60.4° further convinced its preferred *ab*-orientation. On the contrary, for the NiAl-CO₃ LDH (CO₂-satur) layer, the (0 1 2) diffraction peak was totally undetectable (Fig. 3d) and the $I_{(0\ 0\ 3)}/I_{(0\ 1\ 2)}$ ratio reached $+\infty$. Although the relative low crystallinity of LDH crystallites in the NiAl-CO₃ LDH (CO₂-satur) film may affect accurate evaluation of the preferred orientation of LDH films, it was believed that prepared LDH film was still preferentially *c*-oriented to a certain extent since after all, the (012) diffraction peak did not appear in the XRD pattern. The preferred *c*-orientation of the NiAl-CO₃ (CO₂-satur) LDH layer could be further confirmed by its layer-like structure (Fig. 2f). Conventionally, *c*-oriented LDH films could be prepared by physical deposition of pre-formed LDH crystallites on substrates considering their plate-like shapes.¹⁴ Nevertheless, the adhesion between the film and substrate was very weak, making them unsuitable as anti-corrosive coatings.^{6b} In comparison, *in situ* growth method provided better adhesion to the substrate. So far, most of LDH films prepared in this way showed random or *ab*-axis preferred orientation,¹⁵ the preparation of preferentially *c*-oriented LDH films, however, has turned out to be very difficult unless substrates were pre-modified with appropriate organic structure-directing agents.¹⁶ X. Duan et al. reported the *in situ* crystallization of *ab*-oriented and *c*-oriented MgAl-CO₃ LDH films on bare and PVA-modified glass substrates, respectively.¹⁶ The *ab*-oriented LDH film was interpreted by the “evolution selection” growth mechanism. In such case the growth of LDH film was under kinetic control. On the contrary, the formation of preferentially *c*-oriented MgAl-CO₃ LDH film on the PVA-modified glass side was attributed to the strong hydrogen bonding interactions between PVA and MgAl-CO₃ LDH crystallites. The hydrogen-bonding energy, which referred to the thermodynamic parameter, indicated that the film formation process was in fact under thermodynamic control.

It was generally accepted that preferred orientation of inorganic crystalline films was driven by the interaction between thermodynamic and kinetic factors, as in the case of MFI zeolite films.¹⁷⁻²⁰ Based on the previous research, in this study we try to elucidate the change in preferred orientation of NiAl-CO₃ LDH coatings as follow: In most cases *in situ* hydrothermal growth of LDH films is a kinetically controlled process. Under this condition, prepared LDHs film will show *ab*-axis preferred orientation via the “evolution selection” mechanism as in the case of the NiAl-CO₃ LDH (DI aged) coatings. In contrast, formation of *c*-oriented NiAl-CO₃ LDH coatings is a thermodynamically favourable process since the most stable configuration for them to settle onto the surface is to lie on their flat surface (*ab*-face) parallel to substrates. Since concentration of CO₂ in the CO₂-saturated precursor solution is much higher (~ 0.03 M), evolution of the NiAl-CO₃ LDH (CO₂-satur) coatings is no longer under kinetic control and instead, thermodynamic factors gradually dominate the hydrothermal reaction, which ultimately lead to the formation of preferentially *c*-oriented NiAl-CO₃ LDH films.

DC polarization is an effective tool for evaluating anti-corrosive coatings.²¹ In addition to the NiAl-CO₃ LDH (DI

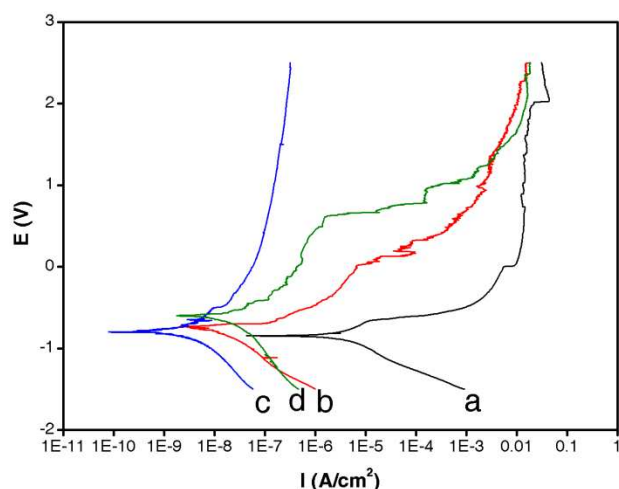


Fig. 4 DC polarization study showing the anodic and cathodic current components of (a) the bare Al substrate, NiAl-CO₃ LDH films prepared from (b) aged DI water and (c) CO₂-saturated water. (d) DC polarization pattern of the NiAl-CO₃ LDH (CO₂-satur) film after immersion in a 3.5 wt.% NaCl aqueous solution for 15 days.

aged) and LDH (CO₂-satur)-modified Al plates, a bare Al plate was also subject to the test for reference. Before the DC experiment, all samples were immersed in a corrosive medium (3.5 wt.% aqueous NaCl solution) for 30 min. The horizontal-like anodic current curve of the Al substrate implied that it readily corroded in the NaCl solution.⁷ The I_{corr} for the bare Al substrate was $\sim 10^{-6}$ A·cm⁻² (Fig. 4a). After coating the Al plate with a NiAl-CO₃ LDH (DI aged) layer, the I_{corr} was reduced by one order of magnitude ($\sim 10^{-7}$ A·cm⁻², Fig. 4b). A further large decrease of I_{corr} to $\sim 10^{-9}$ A·cm⁻² could be achieved with the NiAl-CO₃ LDH (CO₂-satur) coating (Fig. 4c), which was rarely observed previously for simple anion (like CO₃²⁻, NO₃⁻, Cl⁻ and CrO₄⁻) intercalated LDH coatings²² and comparable with various organic anion (like laurate and 8-hydroxyquinoline) intercalated LDH coatings^{4a,22f} (summarized in Table 1). This implied that NiAl-CO₃ LDH (CO₂-satur) layers were competent as high-performance, anti-corrosive coatings. In addition, the much lower I_{corr} for the NiAl-CO₃ LDH (CO₂-satur) film, when compared with the NiAl-CO₃ LDH (DI aged) film, was expected because substantial defects were present in the latter (shown in SI-2).

We further investigated the long-term durability of the NiAl-CO₃ LDH (CO₂-satur) layer against corrosion. Results showed that even after immersion in a corrosive medium (3.5 wt.% NaCl solution) for 15 days, the I_{corr} of the NiAl-CO₃ LDH layer-coated Al plate remained as low as $\sim 10^{-8}$ A·cm⁻² (Fig. 4d). Simultaneously, the surface morphology of the LDH layer after the immersion process was characterized (shown in SI-3). Still no conspicuous cracking was observed in the NiAl-CO₃ LDH (CO₂-satur) layer. In comparison, the bare Al plate had been badly corroded after immersion in the NaCl solution. It was supposed that both the intercalation of carbonate anions and preferred *c*-orientation of the NiAl-CO₃ LDH (CO₂-satur) layer may contribute to the long-term durability.

Strong adhesion of anti-corrosion coatings to the metal surface is of vital importance for their practical applications.^{21a,23} Herein scratch test was employed to evaluate the adhesion strength of NiAl-CO₃ LDH (CO₂-satur) coatings to substrates. It was found that no peeling off or delamination

Table 1 Anti-corrosive capacity of metal and its alloy coated with different LDH films.

LDH Film	I_{corr} bare	I_{corr} modified
	(A·cm ⁻²)	(A·cm ⁻²)
ZnAl-V ₁₀ O ₂₈ LDH-epoxy ^{22a}	10 ⁻⁶	10 ⁻⁷
ZnAl-EDTA LDH-epoxy ^{22b}	4.2×10 ⁻⁷	3.0×10 ⁻⁷
ZnAl-CO ₃ LDH-epoxy ^{22b}	4.2×10 ⁻⁷	3.9×10 ⁻⁷
ZnAl-CrO ₄ LDH-epoxy ^{22b}	4.2×10 ⁻⁷	0.7×10 ⁻⁷
ZnAl-Cl LDH-epoxy ^{22b}	4.2×10 ⁻⁷	2.5×10 ⁻⁷
MgAl-CO ₃ LDH ^{22c}	5.9×10 ⁻⁷	4.5×10 ⁻⁶
MgAl-CO ₃ LDH ^{22d}	6.3×10 ⁻⁶	1.5×10 ⁻⁶
ZnAl-NO ₃ LDH ^{4a}	10 ⁻⁶	10 ⁻⁸
ZnAl-laurate LDH ^{4a}	10 ⁻⁶	10 ⁻⁹
MgAl-CO ₃ LDH ^{22e}	1.9×10 ⁻⁴	4.9×10 ⁻⁶
MgAl-NO ₃ LDH ^{22f}	7.4×10 ⁻⁸	1.1×10 ⁻⁸
MgAl-8HQ LDH ^{22f}	7.4×10 ⁻⁸	0.9×10 ⁻⁹
This work	10 ⁻⁶	10 ⁻⁹

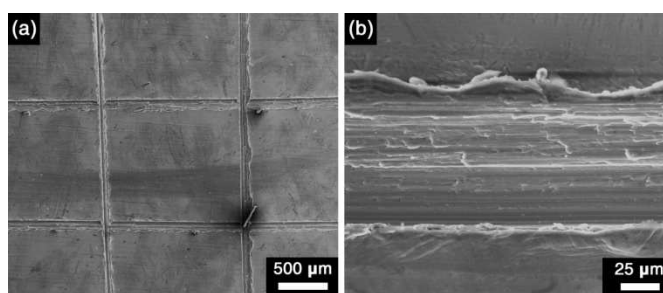


Fig. 5 Evaluation of the adhesion between the NiAl-CO₃ LDH film and Al substrate by scratch test.

occurred after the cross cutting through LDH coatings, which indicated strong adhesion of LDH coatings to aluminium plate surface (Fig. 5). The excellent anti-corrosive capacity, considerable long-term durability as well as strong adhesion of NiAl-CO₃ LDH (CO₂-satur) coatings will make them find wide applications in the field of corrosion protection.

Conclusions

In summary, with the *in situ* hydrothermal method, we successfully prepared anti-corrosive NiAl-CO₃ LDH coatings on aluminium substrates in one step. In particular, it was found that the use of CO₂-saturated water led to the formation of defect-free and preferentially *c*-oriented NiAl-CO₃ LDH layers, which showed excellent anticorrosive performance (polarization current density: $\sim 10^{-9}$ A·cm⁻²), considerable long-term corrosion durability as well as strong adhesion to the substrate. This LDH layer protection technique is simple and eco-friendly, as carbonate intercalated LDHs are conventionally synthesized by precipitation in NaOH-Na₂CO₃ suspension²⁴ or hydrothermal decomposition of urea/HMT.²⁵ Moreover, CO₂, which is also called green gas, is positively utilized. It was further demonstrated that the anti-corrosive capacity of LDH films could be improved not only by appropriate selection of metal ions and charge compensating anions, but also through proper optimization of their microstructure as in the case of zeolite films.^{3a,3b,21}

Acknowledgements

The authors are grateful to the CAS 100-talent program, GZ 911 Sino-German Cooperation Group on Inorganic Membranes, Natural Science Foundation of China (21176231, 21361130018 and 21476223) and Alexander von Humboldt Foundation for the financial support.

Notes and references

^a State Key Laboratory of Catalysis, Dalian Institute of Chemical Physics, Chinese Academy of Sciences, Dalian, 116023, China.

^b Institute of Physical Chemistry and Electrochemistry, Leibniz University Hannover, Callinstr. 3A, D-30167 Hannover, Germany.

^c University of Chinese Academy of Sciences, Beijing, 100039, China.

‡ These authors contribute equally to this work.

Electronic Supplementary Information (ESI) available: [Experimental details: XRD pattern of NiAl-CO₃ LDH powders, magnified cross-sectional SEM images of NiAl-CO₃ LDH films prepared from DI aged and CO₂-saturated precursor solutions, SEM images of the LDH film after long-term corrosion in NaCl solution]. See DOI: 10.1039/b000000x/

- (a) J. Zhao, G. Frankel and R. L. McCreery, *J. Electrochem. Soc.*, 1998, **145**, 2258; (b) L. Xia, E. Akiyama, G. Frankel and R. McCreery, *J. Electrochem. Soc.*, 2000, **147**, 2556.
- (a) S. Pommiers, J. Frayret, A. Castetbon and M. Potin-Gautier, *Corrosion Sci.*, 2014, **84**, 135; (b) S. H. Zaferani, M. peikari, D. Zaarei, I. Danaee, J. M. Fakhraei and M. Mohammadi, *Corrosion*, 2013, **69**, 372.
- (a) R. Cai, M. W. Sun, Z. W. Chen, R. Munoz, C. O'Neill, D. E. Beving and Y. S. Yan, *Angew. Chem. Int. Ed.*, 2008, **47**, 525; (b) Y. J. Dong, Y. Peng, G. L. Wang, Z. B. Wang and Y. S. Yan, *Ind. Eng. Chem. Res.*, 2012, **51**, 3646; (c) M. L. Zheludkevich, R. Serra, M. F. Montemor, K. A. Yasakau, I. M. M. Salvado and M. G. S. Ferreira, *Electrochim. Acta*, 2005, **51**, 208; (d) K. S. Wang, J. Unger, J. D. Torrey, B. D. Flinn and R. K. Bordia, *J. Eur. Ceram. Soc.*, 2014, **34**, 3597.
- (a) F. Z. Zhang, L. L. Zhao, H. Y. Chen, S. L. Xu, D. G. Evans and X. Duan, *Angew. Chem. Int. Ed.*, 2008, **47**, 2466; (b) J. K. Lin, C. L. Hsia and J. Y. Uan, *Scripta Mater.*, 2007, **56**, 927; (c) J. Wang, D. D. Li, X. Yu, X. Y. Jiang, M. L. Zhang and Z. H. Jiang, *J. Alloys Compd.*, 2010, **494**, 271; (d) T. Stimpfling, F. Leroux and H. Hintze-Bruening, *Appl. Clay Sci.*, 2013, **83-84**, 32.
- R. Z. Ma, J. B. Liang, X. H. Liu and T. Sasaki, *J. Am. Chem. Soc.*, 2012, **134**, 19915.
- (a) Q. Wang and D. O'Hare, *Chem. Rev.*, 2012, **112**, 4124; (b) X. X. Guo, F. Z. Zhang, D. G. Evans and X. Duan, *Chem. Commun.*, 2010, **46**, 5197; (c) B. Sels, D. D. Vos, M. Buntinx, F. Pierard, A. K-D. Mesmaeker and P. Jacobs, *Nature*, 1999, **400**, 855; (d) G. R. Williams and D. O'Hare, *J. Mater. Chem.*, 2006, **16**, 3065; (e) S. P. Newman and W. Jones, *New. J. Chem.*, 1998, **22**, 105; (f) V. Rives and M. A. Ulibarri, *Coord. Chem. Rev.*, 1999, **181**, 61.
- X. X. Guo, S. L. Xu, L. L. Zhao, W. Lu, F. Z. Zhang, D. G. Evans and X. Duan, *Langmuir*, 2009, **25**, 9894.
- T. T. Yan, S. L. Xu, Q. Peng, L. L. Zhao, X. H. Zhao, X. D. Lei and F. Z. Zhang, *J. Electrochem. Soc.*, 2013, **160**, C480.
- (a) S. Miyata, *Clays Clay Miner.*, 1983, **31**, 305; (b) Y. Israëli, G. Taviot-Guého, J-P. Besse, J-P. Morel and N. Morel-Frosiers, *J. Chem. Soc. Dalton Trans.*, 2000, 791.
- J. Chen, Y. W. Song, D. Y. Shan and E. H. Han, *Corros. Sci.*, 2012, **65**, 268.
- Y. Liu, N. Y. Wang and J. Caro, *J. Mater. Chem. A*, 2014, **2**, 5716.
- H. Y. Chen, F. Z. Zhang, T. Chen, S. L. Xu, D. G. Evans and X. Duan, *Chem. Eng. Sci.*, 2009, **64**, 2617.
- Z. P. Liu, R. Z. Ma, Y. Ebina, N. Iyi, K. Takada and T. Sasaki, *Langmuir*, 2007, **23**, 861.
- (a) J. H. Lee, S. W. Rhee and D. Y. Jung, *Chem. Commun.*, 2003, 2740; (b) J. H. Lee, S. W. Rhee, H. J. Nam and D. Y. Jung, *Adv. Mater.*, 2009, **21**, 546; (c) R. Z. Liang, R. Tian, W. Y. Shi, Z. H. Liu, D. P. Yan, M. Wei, D. G. Evans and X. Duan, *Chem. Commun.*, 2013, **49**, 969.
- (a) H. Y. Chen, F. Z. Zhang and X. Duan, *Adv. Mater.*, 2006, **18**, 3089; (b) J. H. Lee, S. W. Rhee, H. J. Nam and D. Y. Jung, *Adv. Mater.*, 2009, **21**, 546.
- X. X. Guo, F. Z. Zhang, S. L. Xu, D. G. Evans and X. Duan, *Chem. Commun.*, 2009, 6836.
- S. Li, X. Wang, D. Beving, Z. W. Chen and Y. S. Yan, *J. Am. Chem. Soc.*, 2004, **126**, 4122.
- (a) Z. P. Lai, G. Bonilla, I. Diaz, J. G. Nery, K. Sujatoti, M. A. Amat, E. Kokkoli, O. Terasaki, R. W. Thompson, M. Tsapatsis and D. G. Vlachos, *Science*, 2003, **300**, 456; (b) A. Gouzinis and M. Tsapatsis, *Chem. Mater.*, 1998, **10**, 2497.
- A.-J. Bons and P. D. Bons, *Microporous Mesoporous Mater.*, 2003, **62**, 9.
- (a) Z. B. Wang and Y. S. Yan, *Microporous Mesoporous Mater.*, 2001, **48**, 229; (b) Z. B. Wang and Y. S. Yan, *Chem. Mater.*, 2001, **13**, 1101.
- (a) D. E. Beving, A. M. P. McDonnell, W. S. Yang and Y. S. Yan, *J. Electrochem. Soc.*, 2006, **153**, B325; (b) E. P. Hu, Y. Li, W. Huang, Q. Yan, D. P. Liu and Z. P. Lai, *Microporous Mesoporous Mater.*, 2009, **126**, 81.
- (a) R. G. Buchheit, H. Guan, S. Mahajanam and F. Wong, *Prog. Org. Coatings*, 2002, **47**, 174; (b) T. Stimpfling, F. Leroux and H. Hintze-Bruening, *Appl. Clay Sci.*, 2013, **83-84**, 32; (c) J. Chen, Y. W. Song, D. Y. Shan and E. H. Han, *Corrosion Sci.*, 2011, **53**, 3281; (d) J. Wang, D. D. Li, X. Yu, X. Y. Jing, M. L. Zhang and Z. H. Jiang, *J. Alloy Compd.*, 2010, **494**, 271; (e) F. Z. Zhang, M. Sun, S. L. Xu,

- L. L. Zhao and B. W. Zhang, *Chem. Eng. J.*, 2008, **141**, 362; (f) L. D. Wang, K. Y. Zhang, H. R. He, W. Sun, Q. F. Zong and G. C. Liu, *Surf. Coatings Technol.*, 2013, **235**, 484.
- 23 Y. M. Liu, L. H. Li, X. Cai, Q. L. Chen, M. Xu, Y. W. Hu, T.-L. Cheung, C. H. Shek and P. K. Chu, *Thin Solid Films*, 2005, **493**, 152.
- 24 Z. P. Xu, G. S. Stevenson, C. Q. Lu, G. Q. Lu, P. F. Bartlett and P. P. Gray, *J. Am. Chem. Soc.*, 2006, **128**, 36.
- 25 N. Iyi, K. Tamura and H. Yamada, *J. Colloid Interf. Sci.*, 2009, **340**, 67.